Pergamon

Tetrahedron: *Asymmetry* 10 (1999) 4191–4202

TETRAHEDRON: *ASYMMETRY*

# Switched enantiopreference of *Humicola* lipase for 2-phenoxyalkanoic acid ester homologs can be rationalized by different substrate binding modes

Per Berglund,[a,*] Imre Vallikivi,[b] Linda Fransson,[a] Heinz Dannacher,[c] Mats Holmquist,[a] Mats Martinelle,[a] Fredrik Björkling,[c] Omar Parve [b] and Karl Hult [a]

[a]*Department of Biotechnology, Royal Institute of Technology, SE-100 44 Stockholm, Sweden*

[b]*Department of Bioorganic Chemistry, Institute of Chemistry at Tallinn Technical University, Akadeemia tee 15, Tallinn 12618, Estonia*

[c]*Leo Pharmaceutical Products, Industriparken 55, DK-2750 Ballerup, Denmark*

Received 22 September 1999; accepted 4 October 1999

**Abstract**

*Humicola lanuginosa* lipase was used for enantioselective hydrolyses of a series of homologous 2-phenoxyalkanoic acid ethyl esters. The enantioselectivity (*E*-value) of the enzyme changed from an (*R*)-enantiomer preference for the smallest substrate, 2-phenoxypropanoic acid ester, to an (*S*)-enantiomer preference for the homologous esters with longer acyl moieties. The *E*-values span the range from *E*=13 (*R*) to *E*=56 (*S*). A molecular modeling study identified two different substrate-binding modes for each enantiomer. We found that the enantiomers favored different modes. This discovery provided a model that offered a rational explanation for the observed switch in enantioselectivity. 

## 1. Introduction

Lipases are frequently used in various chemical applications today and more than 30 lipases are commercially available.[1–4] Due to their generally excellent ability in enantiomer discrimination they have a widely recognized potential for the production of enantiomerically pure compounds.[5] They are frequently used both in kinetic resolutions of racemates and in asymmetrizations of prochiral and meso compounds.[6,7] However, identifying the best lipase for a given transformation often leads to a necessary but expensive and time-consuming screening procedure. One approach to overcome this limitation would

* Corresponding author. Tel: +46 8 790 75 12; fax: +46 8 22 46 01; e-mail: per.berglund@biochem.kth.se

0957-4166/99/$ - see front matter 
*PII:* S0957-4166(99)00438-3

be the rational tailoring of enzyme enantioselectivity by protein engineering methods. In order to achieve this, a more detailed knowledge of lipase catalysis on a molecular level is needed.

Chiral carboxylic acids are important building blocks for the synthesis of many pharmaceuticals,[5] pesticides,[8] and natural compounds such as pheromones,[9] where often substances of very high enantiomeric excess (>99.5% ee) are needed. Lipase-catalyzed resolution of racemic carboxylic acids is kinetically more complex than the resolution of racemic alcohols since, in the former case, two diastereomeric acyl enzymes are formed.[10] Hence, both the formation and breakdown of the acyl enzymes pass through transition states that might be involved in defining the enantioselectivity of the resolution of a chiral acid.[11]

Switched enantiomer preference within a homologous series of racemic chiral acyl donors has previously been observed for instance with the serine hydrolase subtilisin.[12] In this case, the existence of two different modes of binding the substrate to the enzyme active site explaining the change in enantiopreference has recently been confirmed by X-ray crystallography using enantiomeric boronic acid inhibitors.[13] In *Candida rugosa* lipase, methyl-branched chiral fatty acids have been used as model compounds and modeling studies have predicted the existence of two different modes of binding of the enantiomers of such a chiral acyl donor to the active site.[14] The fast reacting enantiomer orients its hydrophobic acyl chain into the active-site tunnel, which is a unique feature of this kind of lipase,[15] whereas the slow reacting enantiomer leaves the tunnel empty. The existence of these two substrate-binding modes has recently been experimentally confirmed.[16] Similarly, for *Candida antarctica* lipase B, it has recently been shown that 4-methyl-branched acids can be resolved, and that the enantiomers orient their acyl chain differently in the active site of the enzyme.[17] Two different modes of binding substrate enantiomers have also been described for homologous secondary alcohols with *C. antarctica* lipase B.[18] In this case, longer alcohols have an inverted orientation in the enzyme active site.

*Humicola lanuginosa* lipase (HLL) has a molecular weight of 30 kDa. The X-ray crystal structure of HLL is known.[19] A helix, a lid, covers the superficial active site of the lipase in its closed conformation. HLL is produced recombinantly in extensive amounts (Lipolase®, Novo Nordisk A/S) and can readily be obtained in large quantities and high purity. According to the crystal structure of an HLL–inhibitor complex, the lipase has a hydrophobic crevice, which extends from the active-site serine and accommodates the first seven to eight carbons of the acyl chain.[19] Also, tryptophane 89 (Trp89) in the lid of the lipase has been shown to be important for binding the acyl chain of natural substrates.[20] However, Trp89 has a negative impact on the rate and enantioselectivity in hydrolysis of non-natural substrates such as racemic 2-alkyl substituted alkanoates.[21]

In this work, we are studying lipase catalysis and the lipase enantiomer discrimination processes in detail using rational substrate engineering in combination with molecular modeling. This provides new knowledge of substrate/enzyme interactions and of the mechanisms controlling enzyme enantioselectivity, and will guide future protein engineering attempts for controlling and maximizing selectivity of synthetically useful enzymes.

## 2. Results

Racemic ethyl 2-phenoxyalkanoates **1**–**7**, the related methyl ester **8**, and the phenyl-substituted analog **9** were synthesized from the corresponding 2-bromoalkanoyl esters and phenol in good yields.

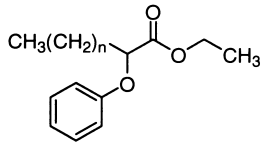

**1**: n = 0
**2**: n = 1
**3**: n = 2
**4**: n = 3
**5**: n = 4
**6**: n = 5
**7**: n = 7

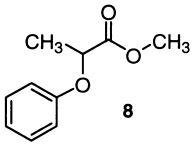

**8**

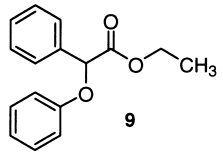

**9**

*Humicola lanuginosa* lipase-catalyzed hydrolyses of **1**–**9** were performed in a pH-stat instrument. The initial rates and enantioselectivity (*E*) displayed by HLL as well as the sign of the optical rotation for the remaining unhydrolyzed substrate are shown in Table 1.

Table 1
Results of the HLL-catalyzed hydrolyses of compounds **1**–**9**

| Substrate | Initial rate [a] (μmol $mg^{-1}$ $min^{-1}$) | *E* | Remaining Ester | | Enantiopreference |
|---|---|---|---|---|---|
| | | | Sign of opt. rot. | Config. | |
| **1** | 190 | 13 | - | S[b,c] | R |
| **2** | 4.5 | 1.5 | + | R[c] | S |
| **3** | 31 | 14 | + | R[c] | S |
| **4** | 18 | 22 | + | R[c] | S |
| **5** | 180 | 56 | + | R[d] | S |
| **6** | 90 | 35 | + | R[d] | S |
| **7** | 25 | 27 | + | R[d] | S |
| **8** | 240 | 14 | - | S[c] | R |
| **9** | 4.6 | 2.0 | - | n.d. | n.d. |

[a] The relative errors were estimated to ±10%.

[b] Absolute configuration (*S*)-(-) of **1** has been reported in the literature (ref 22).

[c] Absolute configuration (*S*)-(-) of the corresponding acid has been reported in literature (ref. 22).

[d] Estimation based on the known configuration of **1**-**4**.

The first seven substrates with increasing acyl chain lengths, **1**–**7**, displayed a gradual change in enantioselectivity with (*R*)-enantiomer preference for **1** switching to (*S*) preference for the substrates with longer acyl chains. Substrate **2** is close to the switch and displayed very low enantioselectivity with (*S*)-enantiomer preference. Changing the alcohol moiety from ethyl in **1** to methyl in **8** had little effect on both the reaction rate and enantioselectivity. The phenyl-substituted **9** was slow and displayed a low enantioselectivity.

The highest *E*-value and a high initial rate were seen with substrate **5**. When a mutant of HLL was used where the tryptophan residue in the lid of the lipase had been replaced with a glycine (HLL-W89G), the initial rate towards **5** increased twofold but the *E*-value remained virtually the same (Table 2).

In order to rationalize the fact that the lipase changed its enantiopreference from (*R*) to (*S*) with an increasing alkyl chain length on the stereocenter (substrates **1**–**7**), a molecular modeling study was undertaken. Initially, two substrates, **1** and **5**, were selected for modeling. These substrates displayed the largest difference in enantioselectivity within the homologous series and represented the extremes of *E*-values with opposite enantiopreference. Substrate **6**, displaying the second highest *E*-value, was included at a later stage to give a larger data set.

Table 2
Hydrolysis of substrate **5** catalyzed by HLL and the mutant HLL-W89G

| Enzyme | Initial rate [a] (μmol $mg^{-1}$ $min^{-1}$) | *E* |
|---|---|---|
| HLL | 180 | 56 |
| HLL-W89G | 360 | 70 |

[a] The relative error in the initial rates was estimated to be ±10 %.

The basis for lipase enantioselectivity is the difference in transition-state energy between the reacting enantiomers.[11] In serine hydrolases the tetrahedral intermediate formed by the substrate after nucleophilic attack by the serine has been used as a model for the transition state of the reaction. An ester substrate with a chiral acyl part forms two diastereomeric acyl enzymes. In the subsequent step a water molecule cleaves the acyl enzyme. In principle, both these steps can contribute to the overall enantioselectivity in the reaction.[23] However, formation of the acyl enzyme can be considered irreversible in a hydrolytic reaction. We thus focused the modeling studies on the acylation step intermediate.

It is important to note that in molecular modeling only one point along a reaction coordinate will be picked from the complete reaction path. The modeler manufactures a starting structure, and then the simulation gives an ensemble of structures for that single point. This means that it is possible to give the system an unrealistic starting structure which is not on the reaction path at all, i.e. starting from an enzyme–substrate complex that is not reachable for a true process. A minimum requirement is thus that effort is put into finding an unstrained starting structure for the modeling. If the achieved ensemble of structures are diverging from the initial structure although the starting complex was tension free, then we are likely to having simulated a non-reachable complex.

Not all of the possible tetrahedral intermediates were considered reactive. In order to be catalytically active, the tetrahedral intermediate was required to form five hydrogen bonds that are necessary for stabilization of the transition state[18] (Fig. 1). Furthermore, it was assumed that an additional hydrogen bond involving the hydrogen on the catalytic histidine would severely influence the catalysis by restricting the transfer of the hydrogen to the leaving alcohol.

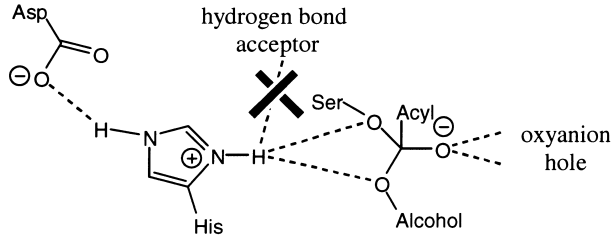


Figure 1. Tetrahedral intermediate of the acylation step used as the transition-state mimic in the molecular modeling studies. The five hydrogen bonds required for catalysis are shown in dashed lines. An additional requirement was imposed in that no additional hydrogen bond (crossed-out) should be formed with the hydrogen on the histidine

To rationalize the observed reversed enantiopreference two questions need to be answered: (i) how do the substrates bind in the active site? and (ii) which enantiomer is the fastest reacting one?

### *2.1. How do the substrates bind in the active site?*

To explore how the tetrahedral intermediates bind in HLL, they were first manually built into the active site. The position of the central part of the substrates was well defined due to the requirement of the formation of catalytic hydrogen bonds. The alcohol part (ethyl) of the substrates was small and had

plenty of space in the alcohol pocket. For the acyl parts of the substrates more considerations had to be made. The acyl parts of the substrates contained the stereocenter with three different groups bound: an alkyl chain of varying lengths, a phenoxy group, and a hydrogen. The acyl-binding site of the HLL active site consists of a large crevice along the surface. From crystal structures of lipase–inhibitor complexes it is known that a crevice is used to accommodate one group from the acyl part of the substrate.[19] Since the acyl part had three different substituents on the stereocenter, there were three possibilities, three *modes*, to position the substrate. In HLL, however, only two modes were possible. The crevice is too narrow to accept a larger group than a hydrogen pointing into its sidewall. This means that the modes with the hydrogen positioned in the crevice would be impossible. Thus, there were two modes, one with the phenoxy group accommodating the crevice, the down mode (with the alkyl chain pointing upwards, out from the enzyme), and the other mode with the phenoxy group pointing upwards, the up mode (the alkyl chain positioned in the crevice) (Fig. 2).

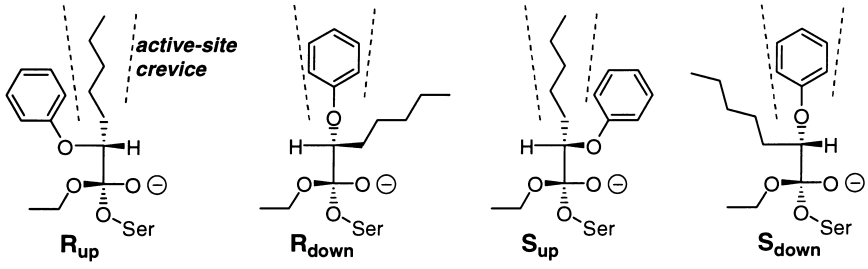


Figure 2. Four combinations of substrate configuration and orientation exemplified for substrate **5**. Index **up** refers to the phenoxy substituent pointing outwards from the enzyme with the acyl chain in the crevice, while **down** means the opposite

To further explore the two modes of substrate binding, dynamics simulations were undertaken for both binding modes of each enantiomer of the three substrates **1**, **5**, and **6**, a total of 12 simulations. When the simulations were examined, it was noticed that the down mode for the (*S*)-enantiomers of all substrates ($S_{down}$) never found a stable conformation. One explanation could be that the conformation forced onto the system by introducing this particular combination of configuration and orientation never would have occurred in reality. This led us to reject the $S_{down}$ mode. Further, the up mode for all (*R*)-enantiomers (as well as $S_{down}$ for **1**) developed a catalytically unfavorable hydrogen bond between the catalytic histidine and the oxygen on the phenoxy group of the substrate. Therefore, the $R_{up}$ binding mode was rejected as well.

The remaining modes were $S_{up}$ and $R_{down}$, and it was then concluded that the (*S*)-enantiomers of the substrates reacted having their phenoxy substituent pointing upwards, while the (*R*)-enantiomers had the phenoxy group in the crevice (Table 3).

### *2.2. Which enantiomer is the fastest reacting one?*

We had a hypothesis where we assumed that each substrate utilizes the binding energy provided by the crevice as much as possible, in accordance with the binding of the inhibitor in the inhibited enzyme.[19] Therefore, it was assumed that for substrate **1**, with a short alkyl chain (methyl), the enantiomer preferring the phenoxy group in the crevice (the down mode) would be favored. For substrates **5** and **6**, however, the binding energy would be best utilized with the more hydrophobic alkyl chains (pentyl and hexyl) accommodated by the crevice and the phenoxy group pointing upwards, the up mode. This assumption predicts a preference of the lipase for the (*R*)-enantiomer for substrate **1** and the (*S*)-enantiomer for substrates **5** and **6**, which is in accordance with the experimental results (Table 1). To support these

Table 3
Evaluation of the 12 simulations

| Substrate | Mode [a] | | | |
|---|---|---|---|---|
| | $R_{up}$ | $R_{down}$ | $S_{up}$ | $S_{down}$ |
| **1** | Additional H-bond between phenoxy oxygen and His258 [b] | OK | OK | Unstable [c] (Additional H-bond) |
| **5** | Additional H-bond [b] | OK | OK | Unstable [c] |
| **6** | Additional H-bond [b] | OK | OK | Unstable [c] |

[a] The indices "up" and "down" refer to the orientation of the phenoxy group relative to the active-site crevice (Figure 2).

[b] "Additional H-bond" means a formed hydrogen bond between the phenoxy oxygen and a proton on the catalytic histidine 258.

[c] "Unstable" implies that a stable conformation was not found, and the conformation would not take place in reality.

arguments, the average potential energies for the last 30 ps of the dynamics simulations were calculated (Table 4). The energies predicted the right enantiomer as well.

Table 4
Average potential energies (without crystal waters) calculated for the last 30 ps of the dynamics simulations for the reactive modes $R_{down}$ and $S_{up}$

| Substrate | Mode | | Preferred enantiomer |
|---|---|---|---|
| | $R_{down}$ (kJ/mol) | $S_{up}$ (kJ/mol) | |
| **1** | -13240 | -13020 | R |
| **5** | -12900 | -13050 | S |
| **6** | -12850 | -13000 | S |

## 3. Discussion

The suggested explanation for the switched enantiopreference can be summarized in three statements: (i) there are two different modes of positioning the substrate in the lipase active site — either the phenoxy group is placed in the crevice (the down mode), or the alkyl chain (the up mode); (ii) the two modes are preferred by different enantiomers — (*R*)-enantiomers react in the down mode and (*S*)-enantiomers in the up mode; and (iii) the enantiopreference of a certain substrate is controlled by optimal utilization of binding energy of the acyl group crevice.

The modeling was performed on the substrates **1**, **5**, and **6**, but the general conclusions could be tested on other substrates as well: the homologous series **1**–**7** was correctly predicted, although no prediction could be made regarding the point where the switch in enantiopreference occurred. Compound **9** was of interest from this point of view. The phenoxy and phenyl groups are very similar. According to the above reasoning, the crevice would probably accommodate the phenoxy group better than

the phenyl, which predicts a down mode from which an (*R*) preference follows. Since the absolute configuration of (−)-**9** is unknown, we could not confirm the predicted enzyme enantiomer preference but the low enantioselectivity (*E*=2) observed was in accordance with the small difference between the two substituents.

Another aspect of the switch in enantiopreference was seen if the data set was arranged to show the free energy difference of the diastereomeric transition state–lipase complexes ($\Delta\Delta G^{\neq}$) as a function of the length of the acyl chain for substrates **1**–**7** (Fig. 3). Increasing the chain length increased the free energy difference between the transition states, but only to a certain degree. Further elongation did not affect the free energy difference markedly.

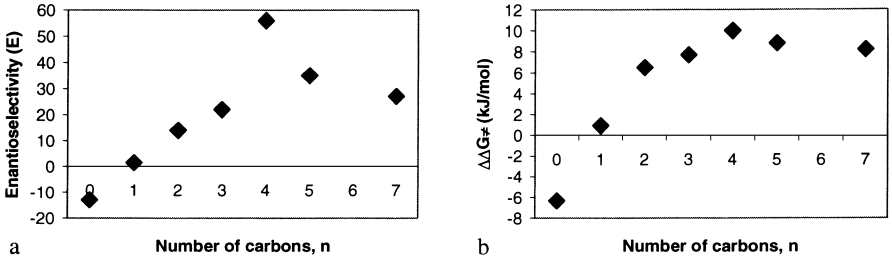


Figure 3. (a) Enantioselectivity *E* as a function of the number of carbon atoms *n*; (b) enantioselectivity expressed as the free energy difference in the transition state ($\Delta\Delta G^{\neq}$=RTlnE). The free energy difference increased with increasing chain length but remained fairly constant after *n*=4 (substrate **5**)

It has been demonstrated that Trp89 in the lid plays a role in the hydrolysis of substrates.[20,21] The activity displayed by the Trp89Gly mutant of HLL for substrate **5** was twofold higher than wild-type HLL (Table 2), but the *E*-value did not change significantly. This can be explained by unfavorable interactions between the side chain of Trp89, covering the active site, and the part of the acyl chain that is directed outwards from the crevice. The unfavorable interaction would be similar for both the (*R*)-enantiomer and the (*S*)-enantiomer of substrate **5**, resulting in similar *E*-values both for wild-type and mutant HLL, but a higher overall activity in the latter case.

## 4. Conclusion

We have shown that the enantioselectivity of HLL is reversed within a homologous series of substrates. Molecular modeling suggests that the (*R*)-enantiomers of all substrates investigated orient their phenoxy substituent in the hydrophobic crevice. In contrast, the (*S*)-enantiomers orient their phenoxy group out from the active site and accommodate their alkyl chain in the crevice. The results from molecular modeling support the hypothesis that the catalytically relevant substrate binding mode giving the optimal interactions with the acyl binding crevice is the favorable one, and is the fast reacting substrate binding mode. Therefore, the switch in enantiomer preference of the enzyme is a consequence of a change of the energetically favorable substrate-binding mode.

Furthermore, we have shown that for *H. lanuginosa* lipase and 2-phenoxycarboxylic acid esters, the highest enantioselectivities were obtained with (*S*) preference for **5** and with (*R*) preference for **1** and **8**. It is notable from the series of homologous substrates that a small change in substrate structure causes a reversed enantiomer preference of the enzyme. These findings will assist future protein engineering work, and they facilitate rational substrate engineering in order to control and maximize enzyme enantioselectivity in synthetic applications.

## 5. Experimental

### 5.1. General

MOPS and gum arabic were purchased from Sigma (St. Louis, MO); ACN from Fisher Scientific (Leicestershire, UK); 1-PrOH, 2-PrOH from Riedel-de Häen (Germany); $NaH_2PO_4 \cdot H_2O$ from J. T. Baker Chemicals B.V. (Deventer, Holland); $Na_2HPO_4 \cdot 12H_2O$, HCl, LiOH, NaOH, and $CaCl_2$ from Merck (Darmstadt, Germany); Na-citrate from Kebo (Stockholm, Sweden). All chemicals used were of analytical or HPLC grade. Silica gel 60 $F_{254}$ pre-coated TLC aluminum sheets from Merck (Darmstadt, Germany) were used. $^1H$ and $^{13}C$ NMR spectra were recorded on a Bruker ARX300 spectrometer at 300 and 75 MHz, respectively, using $CDCl_3$ as solvent and tetramethylsilane (TMS) as internal standard. Mass spectra were recorded at 70 eV using a Micromass, VG Autospec, spectrometer.

### 5.2. α-Substituted carboxylic acids, method A

An equimolar amount of 2-bromoalkanoyl ester, phenol and an excess of $K_2CO_3$ was heated in acetone for about 70 h. The mixture was poured into water and extracted with $Et_2O$, and then washed (NaCl, sat. aq.) and dried.

### 5.3. α-Substituted carboxylic acids, method B

An equimolar amount of 2-bromoalkanoyl ester and potassium phenolate was stirred in DMF at 25°C for 24 h. Workup as above (method A).

### 5.4. α-Substituted carboxylic acids, method C

An equimolar amount of 2-bromoalkanoyl ester, 2-hydroxybenzaldehyde and an excess of $K_2CO_3$ was stirred in DMF at 25°C for 24 h. Workup as above (method A).

### 5.5. Ethyl 2-phenoxypropanoate **1**[24]

Prepared according to method A in 31% isolated yield. $^1H$ NMR δ: 1.22 (3H, t), 1.61 (3H, d), 4.21 (2H, q), 4.74 (1H, q), 6.82 (2H, d), 6.96 (2H, t), 7.27 (1H, t).

### 5.6. Ethyl 2-phenoxybutanoate **2**[25]

Prepared according to method B in 75% isolated yield. $^1H$ NMR δ: 1.08 (3H, t), 1.24 (3H, t), 1.99 (2H, dt), 4.21 (2H, q), 4.55 (1H, t), 6.88 (2H, d), 6.97 (2H, t), 7.26 (1H, t). LRMS *m/z*: 208 ($M^{+\cdot}$), 135, 131, 107, 94, 77.

### 5.7. Ethyl 2-phenoxypentanoate **3**[25]

Prepared according to method A in 39% isolated yield. $^1H$ NMR δ: 0.97 (3H, t), 1.24 (3H, t), 1.57 (2H, m), 1.92 (2H, m), 4.20 (2H, q), 4.60 (1H, dd), 6.86 (2H, d), 6.95 (2H, t), 7.27 (1H, t). HRMS calculated for $C_{13}H_{18}O_3$ ($M^{+\cdot}$): 222.1256; found: 222.1259. LRMS *m/z*: 222 ($M^{+\cdot}$), 149, 129, 107, 94.

### 5.8. Ethyl 2-phenoxyhexanoate **4**[25]

Prepared according to method B in 71% isolated yield. $^1$H NMR δ: 0.92 (3H, t), 1.26 (3H, t), 1.40 (2H, q), 1.50 (2H, m), 1.95 (2H, m), 4.21 (2H, q), 4.60 (1H, dd), 6.87 (2H, d), 6.96 (2H, t), 7.27 (1H, t).

### 5.9. Ethyl 2-phenoxyheptanoate **5**[25]

Prepared according to method B in 92% isolated yield. $^1$H NMR δ: 0.89 (3H, t), 1.24 (3H, t), 1.33 (4H, m), 1.55 (2H, m), 1.93 (2H, m), 4.21 (2H, q), 4.59 (1H, dd), 6.87 (2H, d), 6.96 (2H, t), 7.26 (1H, t).

### 5.10. Ethyl 2-phenoxyoctanoate **6**

Prepared according to method B in 64% isolated yield. $^1$H NMR δ: 0.88 (3H, t), 1.28 (3H, t), 1.33 (6H, m), 1.52 (2H, m), 1.93 (2H, m), 4.21 (2H, q), 4.58 (1H, dd), 6.87 (2H, d), 6.96 (2H, t), 7.26 (1H, t); $^{13}$C NMR δ: 172.0, 158.0, 129.5, 121.5, 115.1, 76.8, 61.1, 32.9, 31.6, 28.9, 25.2, 22.5, 14.2, 14.0. HRMS calculated for $C_{16}H_{24}O_3$ ($M^{+\cdot}$): 264.1725; found: 264.1721. LRMS *m/z* 264 ($M^+$), 191, 171, 97, 94, 55.

### 5.11. Ethyl 2-phenoxydecanoate **7**

Prepared according to method B in 66% isolated yield. $^1$H NMR δ: 0.87 (3H, t), 1.27 (3H, t), 1.29 (10H, m), 1.50 (2H, m), 1.93 (2H, m), 4.21 (2H, q), 4.58 (1H, dd), 6.86 (2H, dd), 6.96 (2H, t), 7.26 (1H, t); $^{13}$C NMR δ: 172.0, 158.0, 129.5, 121.5, 115.1, 76.8, 61.1, 32.9, 31.8, 29.4, 29.2 (2C), 25.2, 22.7, 14.2, 14.1. HRMS calculated for $C_{18}H_{28}O_3$ ($M^{+\cdot}$): 292.2038; found: 292.2040. LRMS *m/z*: 292 ($M^{+\cdot}$), 219, 199, 94, 69, 55.

### 5.12. Methyl 2-phenoxypropanoate **8**[25]

Prepared according to method A in 29% isolated yield. $^1$H NMR δ: 1.61 (3H, d), 3.74 (3H, s), 4.76 (1H, q), 6.85 (2H, d), 6.96 (2H, t), 7.27 (1H, t).

### 5.13. Ethyl 2-phenoxy-2-phenylethanoate **9**[26]

Prepared according to method A in 98% isolated yield. $^1$H NMR δ: 1.18 (3H, t), 4.17 (2H, m), 5.62 (1H, s), 6.95 (3H, m), 7.26 (2H, t), 7.37 (3H, m), 7.58 (2H, d).

### 5.14. Enzymes

Highly purified samples of *H. lanuginosa* lipase and of the Trp89Gly mutant of HLL were from Novo Nordisk A/S, Denmark. The enzyme preparations were pure according to SDS-PAGE (sodium dodecyl sulfate-polyacrylamide gel electrophoresis) with Commassie Blue staining. The enzyme was dissolved in 10 mM MOPS buffer with pH 7.5. Enzyme concentration was determined spectrophotometrically at 280 nm (HLL $\varepsilon=4.3\times10^4$ $M^{-1}$ $cm^{-1}$, HLL-W89G $\varepsilon=3.6\times10^4$ $M^{-1}$ $cm^{-1}$).[21]

### 5.15. Enzymatic hydrolysis of esters

The hydrolyses were run with a pH-stat instrument equipped with an ABU91 Autoburette (1 ml) connected to a VIT90 Video Titrator (Radiometer, Copenhagen). Hydrolysis procedure: The substrate emulsion (1.5 ml, 0.2 M substrate, 5% w/v gum arabicum, 0.2 M $CaCl_2$, pH 7.5) was first emulsified by sonication over 1 min. The reaction was then started by the addition of an enzyme solution to the stirred thermostated substrate emulsion (5–20 μl of an enzyme solution of 0.5–1.0 mg/ml in 10 mM MOPS buffer, pH 7.5). Titration was performed with NaOH (10 or 100 mM) at pH 7.5 and 25°C. The reaction times were 30 min to 6 h. For HPLC analyses, samples (10–30 μl) were withdrawn at different stages of conversion and were added to a water solution of pH 1 in order to stop the reactions.

### 5.16. Determination of enantiomeric excess

Analyses of the enantiomeric excess were performed on a HPLC system equipped with a LC pump (Shimadzu LC6A), a CHIRAL-AGP column 100.4 (ChromTech, Sweden), a UV–vis spectrophotometric detector (Shimadzu SPD-6AV), and an integrator (Perkin–Elmer LCI-100). Also, an HPLC system from Waters was used equipped with a 486 tuneable detector, 600S system controller and a Waters 616 pump. The product/substrate mixtures were extracted from the acidic water phase with diethyl ether. The ether extract was then evaporated and the mobile phase (0.1 M Na-citrate, pH 3.5, or 0.1 M phosphate, pH 7, containing 1–25% of either ACN, 1-PrOH or 2-PrOH) was added to dissolve the product/substrate mixture. The detection was carried out at 225 or 265 nm, depending on the buffer, and the flow rate was 0.9 ml/min. The $ee_s$ and $ee_p$ values were calculated from the base-line separated peak areas. The observed change of enantiopreference was supported by the chiral HPLC analysis. The reacting enantiomer was eluted first for substrate **3** and second for substrates **1** and **8**.

### 5.17. Determination of the optical rotation

The substrate was hydrolyzed to ~40% conversion using the pH-stat, and the remaining substrate and product were extracted from the water phase using diethyl ether. The ether phase was then removed and the extracted substance was flash-chromatographed on silica gel (Merck 60) with *n*-hexane:ethyl acetate (92.5:7.5) as eluent. The purities of the fractions containing the substrate ester were determined by TLC. The signs of the optical rotations of the esters were measured in *n*-hexane at 546 nm using a Perkin–Elmer Polarimeter 241 instrument.

### 5.18. Calculation of E-values

The *E*-values were determined by using the enantiomeric excess ($ee_p$ and $ee_s$) values and conversion values from pH-stat runs. A curve fit of numeric data ($ee_p$, $ee_s$ and/or conversion) was performed by using the program E&K calculator (Anthonsen, H. W. *E&K Calculator*, version 2.03 for Macintosh. For information about the program: http://bendik.mnfak.unit.no), based on the equations by Chen et al.[27,28] For every *E*-value, at least four data points were used for the curve fit.

### 5.19. Molecular modeling

The molecular modeling was based on a crystal structure of HLL[19] with a bound inhibitor showing the lipase in an open conformation. Hydrogens were added to the heavy atoms, and the structure was allowed

to relax in the force field: all enzyme hydrogens were allowed to move during a dynamics simulation of 1000 fs length, and the energy for the hydrogens in the last structure was minimized. The above steps were repeated for the water hydrogens. Then the energy for all hydrogens was minimized and finally the energy of all atoms was minimized. The inhibitor was then removed and replaced with a built substrate. The substrates were assigned empirical charges[29] and atom types consistent with the force field. The substrate was allowed to relax in the enzyme through repeated dynamics simulations and minimizations on subgroups of the substrates: first the hydrocarbon chain in the acyl part of the substrate was allowed to move for 1 ps and the last structure was minimized. Then the phenoxy group, the alcohol group, and finally the whole substrate one at a time were allowed to relax in the same way, whereafter, the energy of the whole system was minimized. The same procedure was repeated for two different conformations of the two enantiomers for three substrates, giving a total of 12 structures. These 12 minimized structures were the starting points for dynamics simulations, lasting for 100 ps each. In the dynamics simulations all atoms were allowed to move. All bond lengths were set to constant values using SHAKE,[30] which made it possible to use a time step of 2 fs. The structure was heated with 50 K per 10 ps up to 300 K, giving a total heating time of 50 ps. All modeling was performed with the software package SYBYL6.5 (Sybyl6.5, Tripos Inc., 1699 South Hanley Rd., St Louis, Missouri, 63144, USA) on an SGI Octane computer. Tripos' implementation of the Amber force field[31,32] considering all atoms was used.

## Acknowledgements

Financial support from the Swedish Council for Forestry and Agricultural Research (SJFR) and from the Swedish National Board for Industrial and Technical Development (NUTEK) is gratefully acknowledged.

## References

1. Wong, C.-H.; Whitesides, G. M. *Enzymes in Synthetic Organic Chemistry*; Pergamon Press: Oxford, 1994.
2. Faber, K. *Biotransformations in Organic Chemistry*, 3rd ed.; Springer-Verlag: Heidelberg, 1997.
3. Kazlauskas, R. J.; Bornscheuer, U. T. In *Biotechnology*, 2nd ed., *Biotransformations I*; Kelly, D. R., Ed. Biotransformations with lipases. VCH: Weinheim, 1998; Vol. 8a, pp. 37–191.
4. Schmid, R. D.; Verger, R. *Angew. Chem., Int. Ed. Engl*. **1998**, *37*, 1609–1633.
5. Zaks, A.; Dodds, D. R. *Drug Discovery Today* **1997**, *2*, 513–531.
6. Johnson, C. R. *Acc. Chem. Res*. **1998**, *31*, 333–341.
7. Berglund, P.; Hult, K. In *Stereoselective Biocatalysis*; Patel, R., Ed. Biocatalytic synthesis of enantiopure compounds using lipases. Marcel Dekker: New York, 1999; pp. 633–657.
8. *Stereoselectivity of Pesticides: Biological and Chemical Problems*; Ariëns, E. J.; van Rensen, J. J. S.; Welling, W., Eds.; Elsevier: Amsterdam, 1988.
9. Högberg, H.-E.; Berglund, P.; Edlund, H.; Fägerhag, J.; Hedenström, E.; Lundh, M.; Nordin, O.; Servi, S.; Vörde. C. *Catal. Today* **1994**, *22*, 591–606.
10. Hult, K.; Holmquist, M. *Methods Enzymol*. **1997**, *286*, 386–405.
11. Sih, C. J.; Wu, S.-H. In *Topics in Stereochemistry*; Eliel, E. L.; Wilen, S. H., Eds.; Wiley: New York, 1989; Vol. 19, pp. 63–125.
12. Martichonok, V.; Jones, J. B. *J. Am. Chem. Soc*. **1996**, *118*, 950–958.
13. Stoll, V. S.; Eger, B. T.; Hynes, R. C.; Martichonok, V.; Jones, J. B.; Pai, E. F. *Biochemistry* **1998**, *37*, 451–462.
14. Holmquist, M.; Hæffner, F.; Norin, T.; Hult, K. *Protein Sci*. **1996**, *5*, 83–88.
15. Grochulski, P.; Bouthillier, F.; Kazlauskas, R. J.; Serreqi, A. N.; Schrag, J. D.; Ziomek, E.; Cygler, M. *Biochemistry* **1994**, *33*, 3490–3500.
16. Berglund, P.; Holmquist, P.; Hult, K. *J. Mol. Catal. B: Enzym*. **1998**, *5*, 283–287.

17. Heinsman, N. W. J. T.; Orrenius, S. C.; Marcelis, C. L. M.; De Sousa Teixeira, A.; Franssen, M. C. R.; Van Der Padt, A.; Jongejan, J.; De Groot, A. *Biocatal. Biotransform*. **1998**, *16*, 145–162.
18. Orrenius, C.; Hæffner, F.; Rotticci, D.; Öhrner, N.; Norin, T.; Hult, K. *Biocatal. Biotransform*. **1998**, *16*, 1–15.
19. Lawson, D. M.; Brzozowiski, A. M.; Rety, S.; Verma, C.; Dodson, G. G. *Protein Eng*. **1994**, *7*, 543–550.
20. Holmquist, M.; Martinelle, M.; Clausen, I. G.; Patkar, S.; Svendsen, A.; Hult, K. *Lipids* **1994**, *29*, 599–603.
21. Martinelle, M.; Holmquist, M.; Clausen, I. G.; Patkar, S.; Svendsen, A.; Hult, K. *Protein Eng*. **1996**, *9*, 519–524.
22. Jacques, J.; Gros, C.; Bourcier, S. In *Stereochemistry. Fundamentals and Methods*; Kagan, H. B., Ed. Absolute configurations of 6000 selected compounds with one asymmetric carbon. Georg Thieme: Stuttgart, 1977; Vol. 4.
23. Hult, K. In *Micobial Reagents in Organic Synthesis*, Servi, S. Ed. A kinetic interpretation of acids and alcohols influence on the enantioselectivity in enzyme catalyzed resolutions. Kluwer Academic Publishers: the Netherlands, 1992; pp. 289–298.
24. Hill, C. M.; Schofield, H. I.; Spriggs, A. S.; Hill, E. *J. Am. Chem. Soc*. **1951**, *73*, 1660–1662.
25. Bomben, A.; Marques, C. A.; Selva, M.; Tundo, P. *Tetrahedron* **1995**, *51*, 11573–11580.
26. Guss, O. *J. Am. Chem. Soc*. **1949**, *71*, 3460–3462.
27. Chen, C.-S.; Fujimoto, Y.; Girdaukas, G.; Sih, C. J. *J. Am. Chem. Soc*. **1982**, *104*, 7294–7299.
28. Chen, C.-S.; Wu, S.-H.; Girdaukas, G.; Sih, C. J. *J. Am. Chem. Soc*. **1987**, *109*, 2812–2817.
29. Berthod, H.; Pullman, A. *J. Chem. Phys*. **1965**, *62*, 942–946.
30. Ryckaert, J. P.; Ciccoti, G.; Berendsen, H. J. C. *J. Comp. Phys*. **1977**, *23*, 327–341.
31. Weiner, S. J.; Kollman P. A.; Case, D. A.; Singh, U. C.; Ghio, C.; Alagona, G.; Profeta, S.; Weiner, P. *J. Am. Chem. Soc*. **1984**, *106*, 765–784.
32. Weiner, S. J.; Kollman, P. A.; Nguyen, D. T.; Case, D. A. *J. Comp. Phys*. **1986**, *7*, 230–252.